Aust. J. Phys., 1986, **39**, 945–59

The Effect of the Flow Distribution on the Thermal Efficiency of a Solar Collector

M. J. O'Keefe and J. L. A. Francey

Physics Department, Monash University,
Clayton, Vic. 3168.

Abstract

An isothermal one-dimensional flow model is used to calculate the flow distribution across the manifold of a flat plate solar collector in order to quantify the effect of a non-uniform flow distribution on the thermal efficiency for a variety of manifold geometries. The predictions of this flow model are found to compare favourably with measured isothermal flow distributions.

1. Introduction

The thermal efficiency of a solar collector is affected by both the total mass flow rate per unit area of absorber plate and the relative mass flow rate through each riser tube of the solar collector. A flat plate solar collector is a special type of heat exchanger and the variation of the thermal efficiency with changes in the mass flow rate, described by the solar collector flow factor F'', can be related to the heat exchanger effectiveness (Phillips 1980):

$$F'' = \mu\{1-\exp(-1/\mu)\}\,; \qquad \mu = m_t\, C_p/F'\, U_t\,, \tag{1a, b}$$

where m_t is the mass flow rate (per unit area of absorber plate) of the heat transfer fluid ($\mathrm{kg\,s^{-1}\,m^{-2}}$), C_p the specific heat of the heat transfer fluid ($\mathrm{J\,kg^{-1}\,K^{-1}}$), F' the solar collector thermal efficiency factor (dimensionless), and U_t the total heat loss coefficient ($\mathrm{W\,m^{-2}\,K^{-1}}$). The factor F'' is calculated by assuming that the mass flow rate through each riser tube is equal. This state of equal flow in each riser tube is defined as a uniform flow distribution, where a flow distribution is described by a set of numbers $V_3(I)$, $I = 1 \rightarrow N$, such that $V_3(I)$ is the mean fluid velocity in the Ith riser tube.

Generally, a solar collector does not have a uniform flow distribution (McPhedran *et al.* 1983), and the local solar collector flow factor F''_I for the Ith riser tube varies for each riser tube. Because F'' varies nonlinearly with m_t in equation (1a), the average solar collector flow factor will be different to that calculated by assuming a uniform flow distribution. Further, since the increased heat loss from the flow starved regions of the absorber plate will be greater than the decreased heat loss from the high flow regions, any deviation from a uniform flow distribution causes a decrease in the thermal efficiency of the solar collector (O'Keefe and Francey 1985).

0004-9506/86/060945$02.00

The temperature variation over the absorber plate of an inclined solar collector will produce buoyancy pressures in the heat transfer fluid. These pressures will be greater in the hotter flow starved regions and, thus, tend to decrease any non-uniformity of the flow distribution if the fluid flow direction is up the inclined absorber plate. The present study of isothermal flow distributions however neglects the effect of buoyancy pressures.

The discrete flow distribution model of Jones and Lior (1978) (a revised version of which has been used in this study) outlined equations to calculate the pressure differential between different branch regions in terms of the flow rates and applied a self-consistent iterative process to calculate the flow distribution. A criticism of this method (McPhedran *et al.* 1983) is that the iterative process limits the number of riser tubes to less than 30 due to the large number of calculations required for convergence. However, with several adjustments, it has been possible to use this method for up to 800 risers with rapid convergence.

In the next two sections, the flow model is outlined and used to quantify the effect of a non-uniform flow distribution on the thermal efficiency of a solar collector.

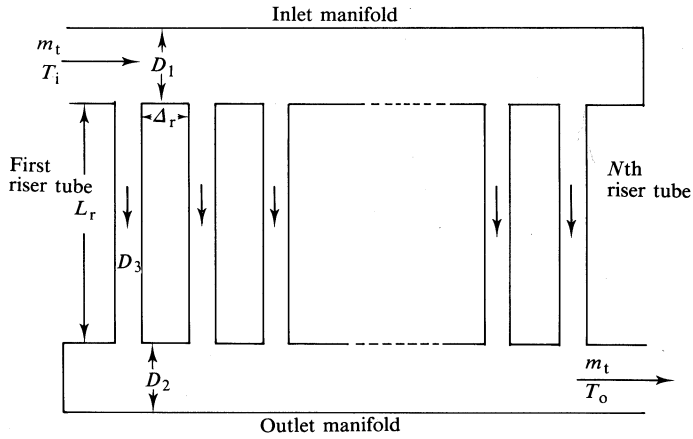

Fig. 1. Geometry of the solar collector.

2. Flow Model

If the heat transfer fluid properties are assumed to be temperature independent and the effect of buoyancy is neglected, the flow distribution will depend on the mass flow rate m_t and the solar collector geometry defined by Δ_r, L_r, D_1, D_2, D_3 and N in Fig. 1. In the flow model it is assumed that the nonlinear flow characteristics at different branch regions are so far removed from each other that there is no interaction, so that flow between different branch regions is isothermal, incompressible and one-dimensional.

The equations governing the pressure differential between branch regions are derived from momentum conservation. As stated by Bajura (1971), there is difficulty in applying energy conservation with the Bernoulli equation 'because of the ambiguity which exists in identifying a relevant streamline on which to conserve energy and estimate frictional losses'. The relevant equations as outlined by Jones and Lior (1978)

are: momentum conservation at the inlet orifice

$$\frac{P_2(J)-P_1(J)}{\rho_1} = V_1^2(J) - V_1^2(J+1) - R_1 \Lambda_i V_1(J) V_3(J); \tag{2}$$

momentum conservation at the outlet orifice

$$\frac{P_4(J)-P_3(J)}{\rho_1} = V_2^2(J) - V_2^2(J+1) - R_2 \Lambda_o V_2(J) V_3(J); \tag{3}$$

pressure drop along the riser tube

$$\frac{P_1(J)+P_2(J)}{\rho_1} - \frac{P_3(J)+P_4(J)}{\rho_1} = (\Psi + f L_r/D_3) V_3^2(J); \tag{4}$$

and pressure drop along the manifold

$$\frac{P_1(J+1)-P_2(J)}{\rho_1} = -\frac{f \Delta_r}{2D_1} V_1^2(J+1), \tag{5a}$$

$$\frac{P_3(J+1)-P_4(J)}{\rho_1} = -\frac{f \Delta_r}{2D_1} V_2^2(J+1); \tag{5b}$$

where

$P_i(J)$ = pressure at different branch regions ($\mathrm{kg\,m^{-1}\,s^{-2}}$)
$V_i(J)$ = fluid velocity in different regions ($\mathrm{m\,s^{-1}}$)
D_1 = inlet manifold diameter (m)
D_2 = outlet manifold diameter (m)
D_3 = riser tube diameter (m)
Δ_r = spacing between adjacent riser tubes (m)
L_r = length of riser tube (m)
N = number of riser tubes
$R_1 = (D_3/D_1)^2$ (dimensionless)
$R_2 = (D_3/D_2)^2$ (dimensionless)
$\Psi = 1 + C_i + C_o$
C_i = turning loss coefficient at inlet branch (dimensionless)
C_o = turning loss coefficient at outlet branch (dimensionless)
Λ_i = static pressure regain coefficient (dimensionless)
Λ_o = static pressure loss coefficient (dimensionless)
ρ_1 = fluid density of heat transfer fluid ($\mathrm{kg\,m^{-3}}$)
f = Moody friction factor corresponding to average fluid speed in a branch region (dimensionless).

The pressures $P_i(J)$ and fluid velocities $V_i(J)$ are shown in Fig. 2.

The first two terms on the right-hand side of equations (2) and (3) represent the induced velocity head, while the third term of (2) describes the effect of axial momentum transport from the inlet manifold fluid stream to the riser tube fluid stream at the branch point. The fluid will lose axial momentum on leaving the branch region of the inlet manifold. On average $V_y = V_3(J)$ (see Fig. 2) from continuity considerations and $V_x < V_1(J)$.

The static pressure regain coefficient Λ_i in equation (2) corrects for the transport of axial momentum into the riser tube and has a value between 0 and 1. Experimental measurement of Λ_i (Bajura 1971) shows that this coefficient is insensitive to changes in the flow ratio $V_3(J)/V_1(J)$ and the diameter ratio R_1, but will increase as Δ_r decreases. The appropriate value for the present study, guided by these measurements, is $\Lambda_i = 0{\cdot}95$.

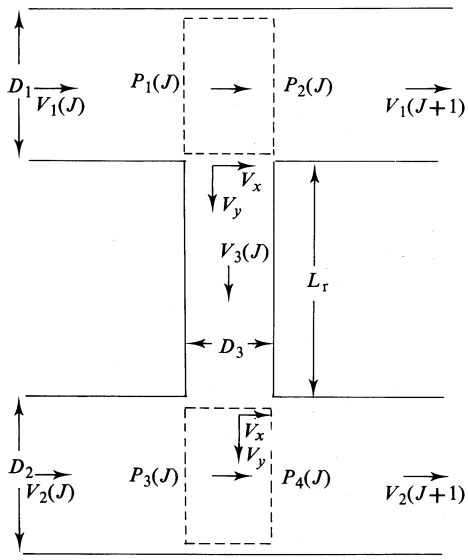

Fig. 2. Branch regions of the solar collector.

The third term on the right-hand side of equation (3) describes the effect of axial momentum transport from the riser tube fluid stream to the outlet manifold fluid stream at the branch point. The mechanism of combining flow is different to diverting flow since the incoming fluid jet from the riser tube penetrates the outlet manifold region where fluid is moving more slowly, causing a flow disturbance. The static pressure loss coefficient Λ_o in equation (3) corrects for the transport of axial momentum from the riser tube and has a value between -1 and 1. The value of Λ_o varies with the ratio R_2 and for this study was taken to be $-0{\cdot}66$, as recommended by Bajura (1971).

The pressure drop along the riser tube in equation (4) is caused by friction loss and the turning pressure loss at the inlet and outlet manifolds, quantified by the coefficients C_i and C_o respectively. The values for this study are $C_i = 0{\cdot}80$ and $C_o = 0{\cdot}90$, as recommended by Bajura (1971). In equation (5), the pressure drop along the manifold between adjacent riser tubes is caused by friction loss.

The Moody friction factor f is given by (McPhedran *et al.* 1983)

$$f = 64/R_e; \qquad 0 < R_e < 2000 \tag{6a}$$

$$= 0{\cdot}0090 + 0{\cdot}0000115 R_e; \quad 2000 < R_e < 4000 \tag{6b}$$

$$= 0{\cdot}0550; \qquad 4000 < R_e, \tag{6c}$$

where $R_e = VD/\nu$ is the Reynolds number, with ν the kinetic viscosity of the fluid ($m^2\,s^{-1}$), D the pipe diameter (m), and V the fluid speed in the region ($m\,s^{-1}$).

Conservation of mass at the branch regions requires

$$V_1(J+1) = V_1(J) - R_1\, V_3(J), \qquad V_2(J+1) = V_2(J) + R_2\, V_3(J). \tag{7a, b}$$

If $V_1(J+1)$ and $V_2(J+1)$ are substituted into equations (2) and (3) we get

$$\frac{P_2(J)-P_1(J)}{\rho_1} = -R_1^2\, V_3^2(J) - (\Lambda_i - 2) R_1\, V_1(J)\, V_3(J), \tag{2'}$$

$$\frac{P_4(J)-P_3(J)}{\rho_1} = -R_2^2\, V_3^2(J) - (\Lambda_o + 2) R_2\, V_2(J)\, V_3(J). \tag{3'}$$

If we assume laminar fluid flow in the riser tube, then equation (6) can be used to calculate f and (4) becomes

$$\frac{P_1(J)+P_2(J)}{\rho_1} - \frac{P_3(J)+P_4(J)}{\rho_1} = \Psi\, V_3^2(J) + \frac{64\nu L_r}{D_3^2}\, V_3(J). \tag{4'}$$

3. Method of Solution

If the values of $P_1(J)$, $P_3(J)$, $V_1(J)$ and $V_2(J)$ in Fig. 2 are known, then equations (2') and (3') can be used to express $P_2(J) - P_4(J)$ in terms of $V_3(J)$. The same can be said for equation (4') so that $P_2(J) - P_4(J)$ can be eliminated and a quadratic in $V_3(J)$ obtained:

$$\frac{P_2(J)-P_4(J)}{\rho_1} = \frac{P_3(J)-P_1(J)}{\rho_1} + \Psi\, V_3^2(J) + \frac{64\nu L_r}{D_3^2}\, V_3(J)$$

$$= \frac{P_1(J)-P_3(J)}{\rho_1} + \{R_2(\Lambda_o+2)\, V_2(J) - R_1(\Lambda_i-2)\, V_1(J)\}\, V_3(J) + (R_2^2 - R_1^2)\, V_3^2(J);$$

$$A_1\, V_3^2(J) + A_2\, V_3(J) + A_3 = 0, \tag{8}$$

where

$$A_1 = R_2^2 - R_1^2 - \Psi, \qquad A_3 = 2\{P_1(J) - P_3(J)\}/\rho_1,$$

$$A_2 = R_2\, V_2(J)(\Lambda_o+2) - R_1\, V_1(J)(\Lambda_i-2) - 64\nu L_r/D_3^2,$$

so that

$$V_3(J) = \{-A_2 \mp (A_2^2 - 4A_1 A_3)^{\frac{1}{2}}\}/2A_1. \tag{9}$$

The physical solution of (9) requires a positive pressure drop in the fluid flow direction for each riser tube. We consider the case when $V_3(J)$ is positive and $R_1 = R_2$. The coefficient A_3 gives the magnitude of the pressure drop along the riser tube and, since $V_3(J)$ is positive, then A_3 must also be positive. The coefficient A_1 equals $-\Psi$ so that only the negative root in (9) will give a positive value of $V_3(J)$.

If reverse flow occurs in the riser tube so that $V_3(J)$ is negative, then A_3 will be negative. The friction and velocity head terms in equations (2)–(9) will reverse sign with $V_3(J)$, but the coefficient Ψ in (4') must be replaced by $-\Psi$. Hence A_1 equals

$+\Psi$ so that if $V_3(J)$ is to be negative, then again, the negative root in (9) must be chosen. The rationale in obtaining a solution for $V_3(J)$ in equation (9) is to always take the negative root but, if $P_1(J) < P_3(J)$, then Ψ is replaced by $-\Psi$ in (8).

Since the pressure difference between two branch regions specifies the flow velocity, the absolute value of pressure is not required and so the pressure $P_1(1)$ at the first riser tube of the inlet manifold can be set to zero. The pressure $P_1(2)$ is not known and a self-consistent iterative procedure must be followed to determine the flow distribution. If the inlet fluid velocity $V_1(1)$ is specified then $V_2(1) = 0$ and $V_2(N+1) = (R_2/R_1)V_1(1)$. Substitution of an approximate value of $P_2(1)$ into equation (9) allows $V_3(1)$ to be calculated. Then the fluid velocities $V_1(2)$ and $V_2(2)$ can be calculated from (7) and the pressures $P_1(2)$ and $P_3(2)$ for the next riser tube from (5). This process can be continued for the N riser tubes and the value of $P_2(1)$ is chosen so that the boundary condition $V_1(N+1) = 0$ is satisfied. This method has only one unknown, while the method of Jones and Lior (1978) iterates all the riser tube velocities $V_3(J)$ until they converge to self-consistent values.

The present method converged for all configurations chosen (manifolds with 800 riser tubes converged after about 10 iterations) and the resultant calculated flow distributions were then used to determine the effect of the mass flow rate and the solar collector geometry on the thermal efficiency of the solar collector, as discussed in the next section.

4. Variation of System Performance with Manifold Parameters

Our flow model can be used to calculate the effect of the flow distribution on the thermal efficiency of a solar collector, described by the Hottel–Whillier–Bliss equation (Duffie and Beckman 1980)

$$\eta = F''F'\{\tau\alpha - U_t(T_i - T_e)/G_t\}, \tag{10}$$

where $\tau\alpha$ is the transmission–absorptance coefficient (dimensionless), T_i the inlet temperature of the heat transfer fluid (K), T_e the equivalent environmental sink temperature (K), and G_t the total incident solar radiation ($W\,m^{-2}$), with the solar collector flow factor F'' (denoted below by F''_{un}) calculated assuming a uniform flow distribution. The parameter of interest when studying non-uniform flow distributions is the change in the thermal efficiency of the solar collector. If the heat loss coefficient U_t and the solar collector efficiency factor F' are assumed to apply locally for each riser tube, the local solar collector flow factor F''_J for the Jth riser tube can be calculated from the mean fluid velocity $V_3(J)$ as

$$F''_J = \mu_J\{1 - \exp(-1/\mu_J)\}; \qquad \mu_J = \frac{\rho_1 C_p \tfrac{1}{4}\pi D_3^2 V_3(J)}{U_t F' L_r(\Delta_r + D_3)}, \tag{11a, b}$$

so that the average thermal efficiency is

$$\eta = \frac{1}{N}\sum_{J=1}^{N}\eta_J = F'\{\tau\alpha - U_t(T_i - T_e)/G_t\}\frac{1}{N}\sum_{J=1}^{N}F''_J,$$

and the average flow factor is

$$F''_{av} = \frac{1}{N}\sum_{J=1}^{N}F''_J. \tag{12}$$

By using the flow model outlined in the previous section to calculate the flow distribution, the average flow factor (12) can be calculated for a specified mass flow rate and solar collector geometry. The independent variables chosen to classify the solar collector geometry were the manifold diameters D_1 and D_2, the riser tube length L_r and the number of riser tubes N. For each set of these parameters, the average solar collector flow factor ratio

$$F''_{fr} = F''_{av}/F''_{un} \tag{13}$$

was used as the only parameter to classify the system. Thus, the effect of the mass flow rate and the solar collector geometry on the thermal efficiency can be quantified by the single parameter F''_{fr}. The variation of F''_{fr} with each parameter was examined independently, where the default values of the other parameters (unless specified) are shown in Table 1. The values of D_3, Δ_r, F' and U_t chosen are shown in Table 2 and are typical for a glazed flat plate solar collector with an EPDM rubber absorber plate.

Table 1. Default solar collector geometry and mass flow rate

D_1 (m)	D_2 (m)	L_r (m)	N	m_t (kg m^{-2} s^{-1})
0·024	0·024	5·0	500	0·015

Table 2. Constant parameters

D_3 (m)	Δ_r (m)	F'	U_t (W m^{-2} K^{-1})
0·0047	0·008	0·93	9·0

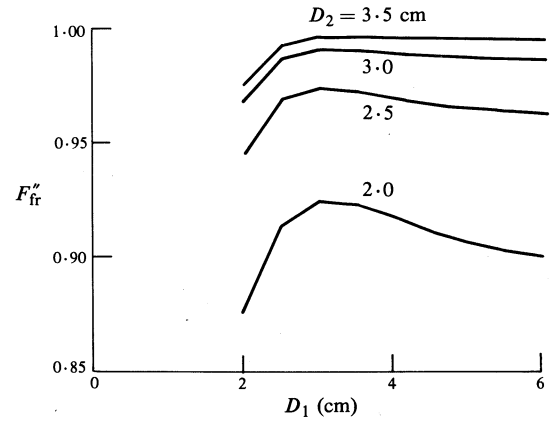

Fig. 3. Variation of F''_{fr} with the manifold diameters D_1 and D_2.

Since the magnitude of the pressure differential across the riser tube reflects the magnitude of the riser tube fluid velocity, a uniform flow distribution requires that the variation of pressure along the manifolds is much less than the average pressure differential across the riser tubes. The pressure variation along the inlet manifold will be determined by the interplay between the friction loss and the induced velocity head in equation (2). When the fluid velocity is large at the start of the inlet manifold, the

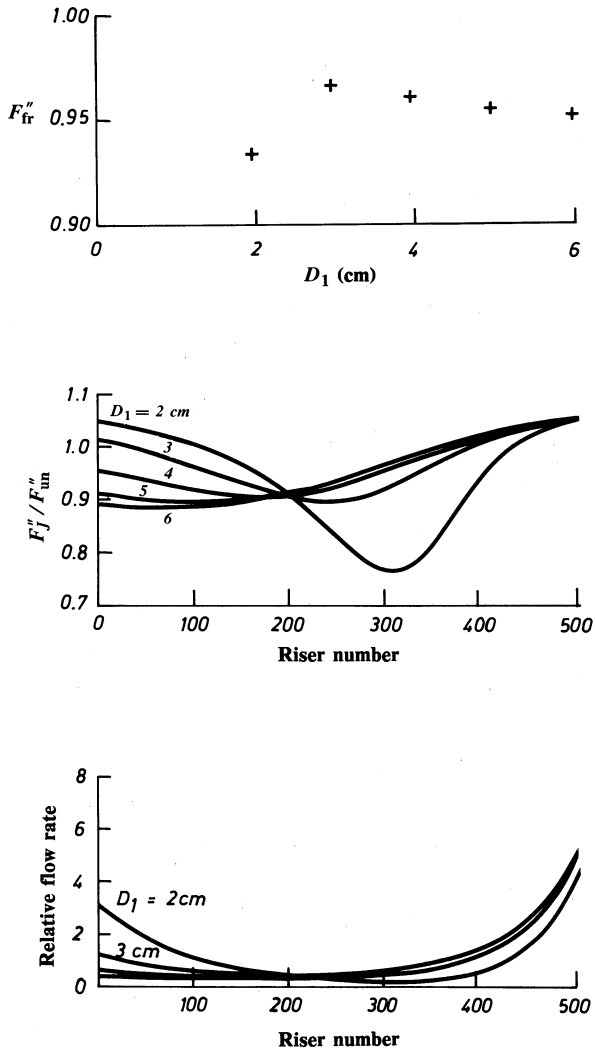

Fig. 4. Effect of the inlet manifold diameter D_1 on the flow distribution: variation of the average flow factor ratio with D_1 (*top*); variation of the local flow factor ratio along the manifold (*middle*); and variation of the relative flow rate along the manifold (*bottom*).

friction loss term dominates and the pressure decreases along the inlet manifold with increasing riser tube number. As the fluid velocity decreases along the inlet manifold, the induced velocity head term dominates and the pressure begins to increase along the inlet manifold with increasing riser tube number. The friction loss and induced velocity head terms in equation (3) combine causing a decrease in pressure along the outlet manifold with increasing riser tube number. The pressure variation along the inlet and outlet manifolds will increase with the fluid velocity which increases when m_t increases or D_1 or D_2 decreases.

The variation of F''_{fr} with the manifold diameters D_1 and D_2 is shown in Fig. 3, indicating that values of D_1 and D_2 greater than 3 cm avoid a decrease in the thermal efficiency due to a non-uniform flow distribution.

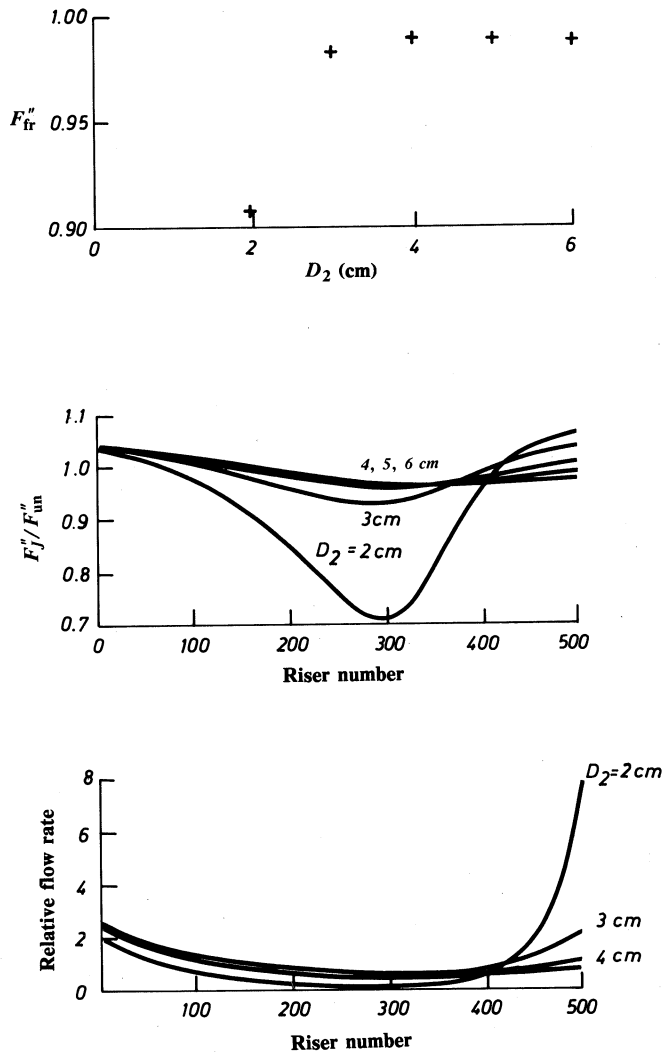

Fig. 5. Effect of the outlet manifold diameter D_2 (see caption to Fig. 4).

Figs 4 and 5 show F''_{fr}, F''_J/F''_{un} and the relative flow rate for different values of D_1 and D_2 respectively. The relative flow rate in the Jth riser tube is $V_3(J)/\langle V_3(J)\rangle$, where $\langle V_3(J)\rangle$ is the mean riser tube velocity.

Fig. 6 shows that an increase in the mass flow rate m_t increases the non-uniformity of the flow distribution and hence decreases F''_{fr} due to the higher fluid velocities in the solar collector. When the number of riser tubes N is increased, as in Fig. 7, the length of the manifolds and hence the pressure variation along the manifolds increases. Also, since the solar collector area has increased, the fluid velocity in the manifolds increases. This causes an increase in the non-uniformity of the flow distribution and hence a decrease in F''_{fr}.

Fig. 8 shows that there is no change in F''_{fr} or the flow distribution as the riser tube length L_r increases for the range of L_r examined. The pressure differential across the riser tubes increases as L_r increases but, since the solar collector area has

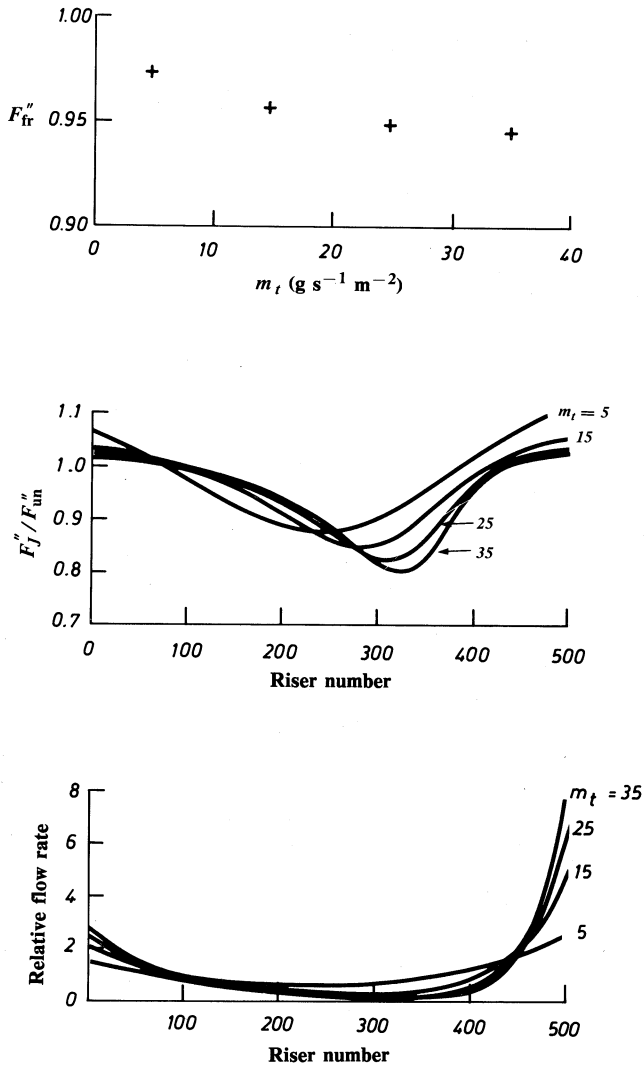

Fig. 6. Effect of the mass flow rate m_t (see caption to Fig. 4).

increased, the fluid velocity in the manifold increases to counter this effect. Thus, for the range of solar collector parameters considered, this study recommends that the solar collector be installed with a large value of L_r and a correspondingly smaller value of N for a given solar collector area. This would also simplify the installation of the solar collector due to the smaller number of connections required between the manifolds and the riser tubes.

Figs 4–8 illustrate the effect of varying the parameters D_1, D_2, m_t, N and L_r on the thermal efficiency of a solar collector. Due to the numerical nature of this study, trends can only be discussed for the parameters listed in Tables 1 and 2. While we have confined these parameters to be relevant to EPDM rubber absorber plates, the flow model is equally relevant for different manifold systems and so the parameters in Tables 1 and 2 can be varied accordingly.

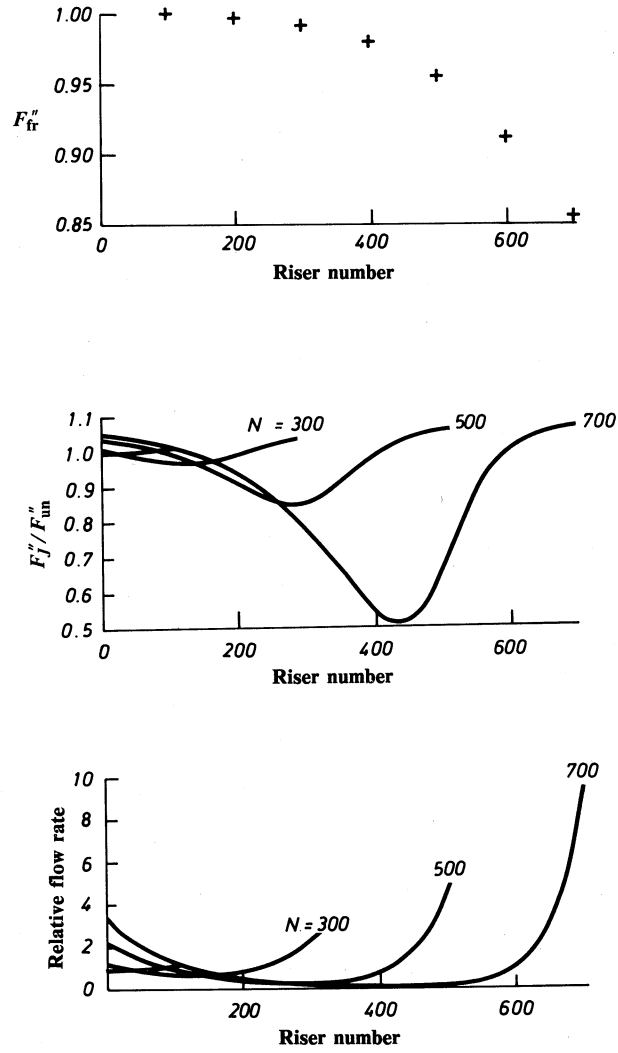

Fig. 7. Effect of the riser tube number N (see caption to Fig. 4).

5. Flow Measurement

Manometers were used to measure the pressure drop across each riser tube which varies linearly with the mass flow rate in the laminar flow regime (for all measurements flow in the manifolds and riser tubes was in the laminar flow regime). The pressure drop across the riser tube ∂P for the flow rates of interest was equivalent to a head of several centimetres of water. Since ∂P is so small, any variation across the manifold would be impossible to measure unless ∂P was amplified.

The pressure drop along the riser tube due to friction is given by, similar to equation (4),

$$-\frac{\partial P}{L_r} = \frac{8\nu\rho_1 V_r}{D_3^2} = \frac{(\rho_2-\rho_1)g\Delta h}{L_r}, \tag{14}$$

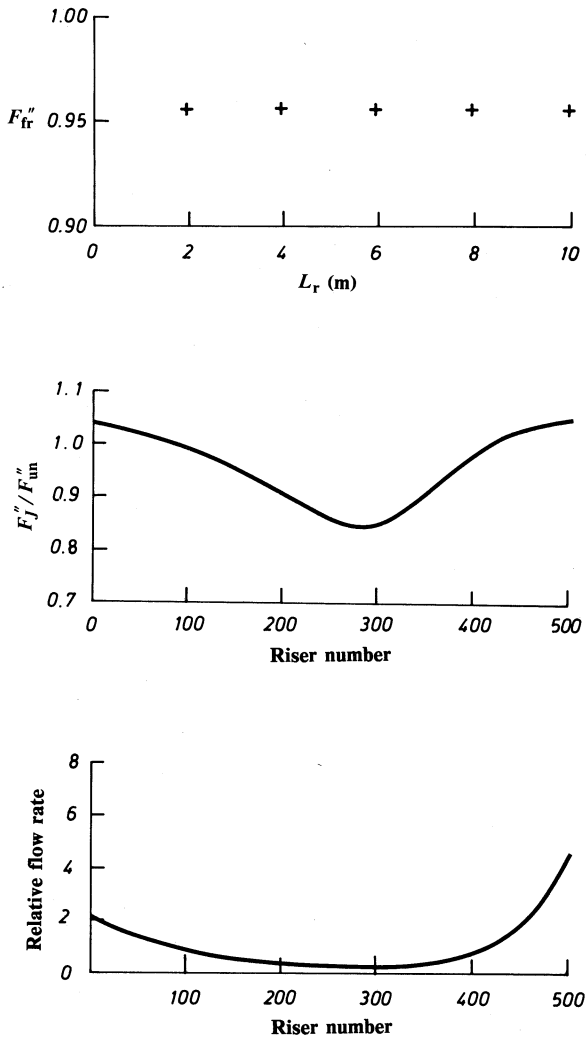

Fig. 8. Effect of the riser tube length L_r (see caption to Fig. 4).

where V_r is the fluid speed in the riser tube ($m\,s^{-1}$), ρ_2 the density of the manometer fluid ($kg\,m^{-3}$), Δh the height differential on the manometer (m), and g the gravitational constant ($m\,s^{-2}$).

One of the fluids to be used in the manometer is obviously water, while the other must have the following features:

(a) be insoluble in water;

(b) have a refractive index different from that of water to observe the meniscus;

(c) have a density slightly greater than water;

(d) be relatively inexpensive and easy to obtain.

There are many organic fluids which satisfy these requirements. Some of these fluids however will attack PVC and brass fittings, and so the manometers were constructed from glass tubing. Butyll chloride ($\rho_2 = 1{\cdot}12\,kg\,m^{-3}$) proved especially suitable and all experimental data reported here were obtained using this fluid.

The experimental collector was assembled using EPDM mats which, as supplied, are about 10 cm wide and consist of a flat sheet (back-plate) on which six riser tubes lie. The assembly is extruded in one piece and the mat may be cut to any desired length. The riser tubes have a nominal internal diameter of 4·7 mm and are spaced at 8 mm intervals with a 12 mm flap at each side of the mat. Four mats were used to form a collector containing 24 riser tubes not all equally spaced, because of the side flaps, so that every sixth tube was separated from the succeeding tube by three intertube spaces. The riser tubes were connected directly to manifolds at top and bottom. Tests were conducted with inlet and outlet manifold flows in the same direction (parallel flow) and in the opposite direction (antiparallel or reverse flow).

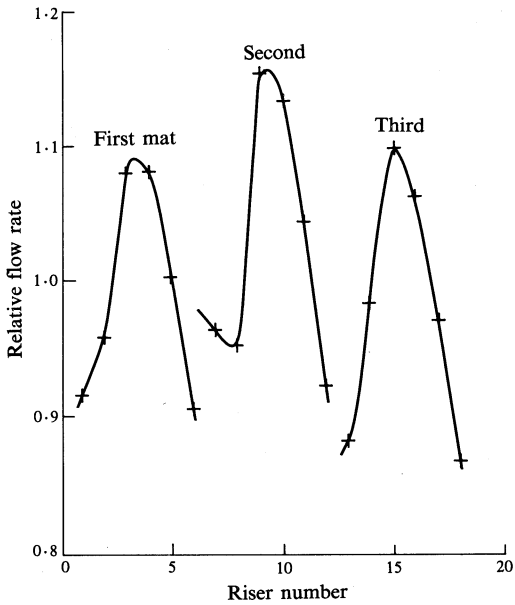

Fig. 9. Flow distribution for EPDM rubber mats.

It was found that there was considerable variability in tube diameter between different mats giving changes in mass flow rate in different risers, depending on which mat was used (see Fig. 9). Since this introduced another variable the mats were replaced by PVC tubing of uniform diameter placed in exactly the same configuration as before. Typical results are shown in Fig. 10 where the *relative* flow rate is plotted against riser number for three different manifold diameters. These figures give a direct picture of the uniformity of the flow as measured and as predicted by the model. In Fig. 10*a* it is clear that the inlet manifold had been cut too short and flow by-passes the first three risers. The model, of course, assumes fully developed laminar flow throughout. The agreement between the predictions and measurements is good. The inter-riser gap after every sixth riser produces the small steps apparent in the measured and predicted results. As shown in Fig. 10*c*, the improvement on changing to larger diameter manifolds is marked. The improvement for antiparallel flow is probably a feature of the particular collector configuration used and this should not be expected for other configurations.

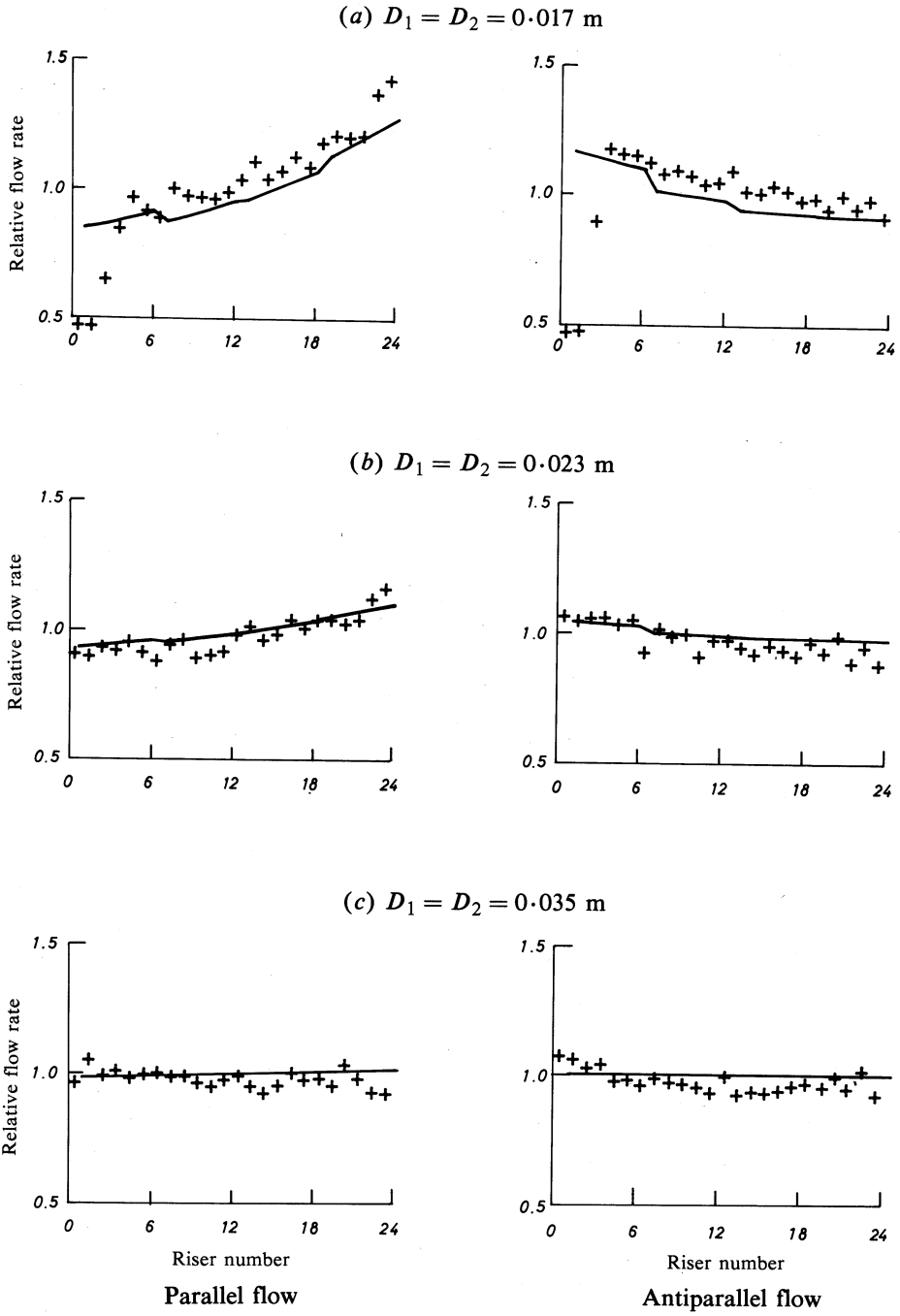

Fig. 10. Several typical measured (crosses) and calculated (curves) relative flow rates for the three values of $D_1 = D_2$ indicated. Parallel and antiparallel flow are shown on the left and right respectively.

6. Conclusions

The parameter F''_{fr}, which quantifies the effect of a non-uniform flow distribution on the thermal efficiency, was examined for a variety of mass flow rates and solar collector geometries. This parameter is most sensitive to the manifold diameters and the number of riser tubes. For the range of parameters examined, this study indicates that the ratio of manifold to riser tube diameters should be greater than six, and the riser tube length should be greater than the length of the manifolds to avoid a significant decrease in the thermal efficiency due to a non-uniform flow distribution.

Acknowledgment

M. J. O'Keefe gratefully acknowledges the financial support of a Monash University Graduate Scholarship.

References

Bajura, R. A. (1971). *J. Eng. Power* **93**, 7–12.

Duffie, J. A., and Beckman, W. A. (1980). 'Solar Engineering of Thermal Processes' (Wiley: New York).

Jones, G. E., and Lior, N. (1978). Isothermal flow distribution in solar collectors and collector manifolds. Proc. Ann. Meet. American Sect. ISES, Denver (ISES: Denver).

McPhedran, R. C., Mackey, D. J., McKenzie, D. R., and Collins, R. E. (1983). *Aust. J. Phys.* **36**, 197–219.

O'Keefe, M. J., and Francey, J. L. A. (1985). *Aust. J. Phys.* **38**, 233–7.

Phillips, W. F. (1980). *Sol. Energy* **24**, 601–2.

Manuscript received 10 February, accepted 10 June 1986